Chinese Journal of Polymer Science Vol. 33, No. 5, (2015), 697−708

Chinese Journal of Polymer Science
© Chinese Chemical Society
Institute of Chemistry, CAS
Springer-Verlag Berlin Heidelberg 2015

Effects of Nanosilica on Crystallization and Thermal Ageing Behaviors of Polyethylene Terephthalate*

Ying-jie Xu, Yi-hu Song** and Qiang Zheng
MOE Key Laboratory of Macromolecular Synthesis and Functionalization, Department of Polymer Science and Engineering, Zhejiang University, Hangzhou 310027, China

Abstract The effects of nanosilica (SiO_2) on crystallization and thermal aging behaviors of polyethylene terephthalate (PET) have been studied using differential scanning calorimetry (DSC) and polarized optical microscopy (POM), viscometry, tensile testing and scanning electron microscopy (SEM). For non-isothermal and isothermal crystallizations, the crystallization rate of PET increases considerably with increasing content of SiO_2 providing a large number of nucleation sites, but the relative crystallinity of the nanocomposites has little differences with that of neat PET. According to POM observation, the nucleation of PET becomes faster and the nucleation density increases significantly with increasing SiO_2 content. For PET and its nanocomposites thermally aged at 190 °C, the results of intrinsic viscosity, carboxyl content and tensile test show that the degradation rate of PET is reduced with the addition of a small content of SiO_2, but the degradation rate increases with further addition of SiO_2, owing to the dual effect of SiO_2 on PET degradation.

Keywords: Polyethylene terephthalate; Nanosilica; Crystallization; Thermal ageing.

INTRODUCTION

Polyethylene terephthalate (PET) has excellent mechanical properties, resistance to fatigue, high rigidity and is widely used in areas of films, fibres and engineering plastics[1, 2]. However, PET has low crystallization rate and poor ageing resistance, which affect its processing and high performance applications[3]. The biaxially stretched PET films could be used at 120 °C for a long period and at 150 °C for a short period and is extensively used as electrically insulating films. In recent years, accompanied with the development of electrical or electronic parts, there are demanding requirements such as excellent thermal stability for the insulation material at higher temperatures.

However, the polar ester groups in PET molecular main chains can easily cause the chains to degrade under different conditions. Pure PET films have poor thermal stability, and thermal aging at 50 °C even causes significant reduction in extensibility. Even in the absence of light, reactive ions and chemical reagents, the life-time of the films may be greatly reduced under combined effect of heat and oxygen which causes thermal, thermal-oxidative and hydrolytic degradations[4]. Especially at high temperatures in the presence of oxygen, the synergistic action of these two factors leads to polymer degradation, which is frequently the main cause of the final breakdown of insulating devices[5]. Many mechanisms have been suggested for thermal and thermal-oxidative degradations, and random chain-scission is the most widely accepted mechanism[6−8]. During degradation, the macromolecules break down into segments terminated with vinyl and carboxyl groups, which causes the materials colouring, bubbling and brittling[9].

* This work was financially supported by the Jiangsu Yuxing Film Technology Co. Ltd., China.
** Corresponding author: Yi-hu Song (宋义虎), E-mail: s_yh0411@zju.edu.cn
Received August 19, 2014; Revised October 3, 2014; Accepted November 15, 2014
doi: 10.1007/s10118-015-1619-x

In last few decades, nanocomposite technology has proved to be an effective way to improve physical properties of polymers[10–18]. Furthermore, nanofillers have been recently shown to improve thermo-oxidative stability of PET. For example, exfoliated graphite could noticeably increase thermal stability of PET nanocomposites prepared by melt-compounding, and the thermo-oxidative degradation temperature at 30% weight loss is improved by 32 K at 7.0 wt% graphite[19]. Addition of organically modified montmorillonite leads to a stabilization effect to PET in the nanocomposites by *in situ* polymerization[20] and significantly improves thermal degradation onset temperature and thermal deformation temperature[21]. Montmorillonite may reduce the degradation onset temperature under nitrogen because of the clay catalysis effect but favors thermo-oxidative stability due to clay barrier effect hindering oxygen to diffuse in[22]. In addition, nanosized silica (SiO_2) could improve the thermal stability[23, 24], activation energies of decomposition and the residual carbon content due to adsorption of the decomposed products on the surface of silica[25]. The formation of a char layer may prevent oxygen and heat permeations into the material. However, Kusuktham[26] found that SiO_2 could improve the char amount without influence the temperatures at 10% and 50% mass losses of composite fibers prepared by melt-spinning. Vassiliou[20] also found that SiO_2 has a negligible effect on the thermal degradation of PET in the nanocomposites by *in situ* polymerization.

The nanofillers also influence the crystallization and melting behaviors of PET while the investigation results are controversial depending on the preparation method and silica content and dispersion. Yang *et al.*[27] demonstrated that SiO_2 could increase crystallization rate and reduce spherulite size and surface free energy for nucleus formation. SiO_2-polystyrene core-shell particles could also reduce crystallization activation energy of PET in both isothermal (200–212 °C) and non-isothermal crystallizations[28]. In PET/SiO_2 nanocomposites by *in situ* polymerization, crystallization rate increases significantly while relative crystallinity (X_c) decreases with increasing silica content[29]. In PET/SiO_2 nanocomposites prepared by cryomilling that causes amorphization of crystalline PET matrix and reduction of molecular weight, SiO_2 particles play a role of nucleating agent to improve the melt crystallization ability, causing X_c and crystallization temperature (T_c) to increase by 30.5% and 35.2 K, respectively[30]. In PET/SiO_2 nanocomposites *via* sol-gel method, SiO_2 depresses non-isothermal crystallization and causes reductions in T_c, melting point (T_m) and X_c[17]. Turturro *et al.*[31] found that less than 1 wt% silica causes a remarkable increase in crystallization rate while silica at higher loadings causes the overall crystallization rate to decrease to values even lower than that of pure PET. The retardation in rate in spite of an increase in density of spherulites is attributed to an increase in melt viscosity due to strong adsorption of polymer segment onto surface of silica particles. The same is found in *in situ* polymerized nanocomposites, where addition of less than 3 wt% SiO_2 could increase non-isothermal T_c and T_m of PET while both T_c and T_m are reduced at 4 wt% SiO_2[32]. Zheng and Wu[33] argued that, during PET non-isothermal crystallization, nanosilica may not behave as a nucleating agent but rather retards the appearance of the microcrystalline phase. It is still lack of consensus about the influence of silica nanoparticles on the crystallization behavior of PET.

The previous investigations show that nanoparticles can be used to mediate the crystallization behavior of PET. It is expected that well dispersed nanosilica particles could nucleate PET macromolecules to form fine crystallites, and both the nanoparticles and the crystallites may restrain the oxygen and moisture diffusion so as to improve the thermo-oxidative aging behavior. But few researchers studied the relation between crystallization behavior and aging behavior of PET/SiO_2 nanocomposites at rather high temperatures.

In addition, although thermal stability of PET/SiO_2 nanocomposites has been studied by some researchers, the previous investigations were almost carried out using the method of dynamic thermogravimetric analysis, which can just study dynamic thermal stability of PET. However, there are few reports about the long-term thermo-oxidative aging of PET/SiO_2 nanocomposites at rather high temperatures. This article aims to systematically investigate the crystallization and isothermal thermo-oxidative ageing behavior of PET/SiO_2 nanocomposites to provide a general understanding of the effect of the nanoparticles and the crystallites on the high-temperature degradation of PET materials.

EXPERIMENTAL

Materials

Poly(ethylene terephthalate) (PET) with an intrinsic viscosity [η] of 0.65 dL·g^{-1} was acquired from Yizheng Petrochem., China. γ-Methacrylic propyl trimethoxysilane (MPS) modified fumed silica nanoparticles (SiO_2) with an average primary particle size of 30 nm and a specific surface area of 200 m^2·g^{-1} was supplied by Hangzhou Wangjing New Mater. Co. Ltd., China.

Preparation of PET/SiO_2 Nancomposite Films

The PET pellets and the SiO_2 powders were dried in a vacuum oven at 120 °C for 4 h. PET and its nanocomposites with 0.5 wt% (PET-0.5) and 1 wt% SiO_2 (PET-1.0) were mixed using a twin-screw extruder (NFM 26SS) at 270 °C for 5 min at a screw rate of 500 r·min^{-1}. The extruded pellets were stretched in a biaxial stretcher at 125 °C with 800 %/min stretch rate in both axes and the stretched films were rapidly roll-cooled to room temperature.

Ageing Treatment

The long-term ageing treatment was performed in a thermostatic container (MT3065, Guangzhou ESPEC Environmental Equipment Co., China) at 190 °C in air environment for different times.

Crystallization Behavior Analysis

DSC measurements

Differential scanning calorimetry (DSC) (Q100, TA, USA) was used to investigate the isothermal and non-isothermal crystallizations of 8–10 mg samples sealed in an aluminium pan. For isothermal crystallization measurements, the samples were heated at a rate of 10 K·min^{-1} to 285 °C, held for 5 min, and then cooled at a cooling rate (Φ) of −50 K·min^{-1} to predetermined temperatures 225 °C, 230 °C, 235 °C and 240 °C for full crystallization. Avrami equation[34, 35] was also used to analyze the PET crystallization kinetics.

$$\lg[-\ln(1-X_t)] = \lg K + n\lg t \tag{1}$$

Here X_t is relative crystallinity at crystallization time t, k is kinetic constant, and n is Avrami exponent reflecting the mechanisms of crystal nucleation and growth.

For non-isothermal crystallization, the samples were heated to 285 °C at a rate of 10 K·min^{-1}, held for 5 min, and were then cooled to room temperature at Φ = 2.5, 5.0, 7.5 and 10 K·min^{-1}, respectively. The non-isothermal crystallization dynamics was analyzed using Jeziorny equation[36].

$$\lg[-\ln(1-X_t)] = \lg Z_t + n\lg t \tag{2}$$

The Avrami index n and crystallization rate constant Z_t could be determined from the slope and the interception on the plot of lg[−ln(1−X_t)] versus lg$t$.

Polarized microscopy

The morphology of crystals was observed using a polarized microscope (POM) attached with heating platform of Linkam-TMS600, Olympus-BX51. The samples were melted in the platform at 300 °C for 5 min and then quickly cooled to 240 °C to crystallize.

Ageing Properties Analysis

Intrinsic viscosity measurements

Intrinsic viscosity [η] measurements were performed with an Ubbelohde viscometer at 25 °C in a mixture of phenol and tetrachloroethane (50/50, *W*/*W*). The solutions were kept at 120 °C for 20 min and were cooled to room temperature followed by filtration through a disposable membrane filter (Teflon). [η] of each sample was calculated using Solomon-Ciuta[37] equation for single point measurement:

$$[\eta] = \left[2\left(\eta_{sp} - \ln\eta_{rel}\right)\right]^{0.5} / \boldsymbol{c} \tag{3}$$

Here, η_{sp} and η_{rel} are specific viscosity and relative viscosity, respectively, and c is mass concentration. Some aged samples were partially insoluble in the above solvent mixture. In these samples, the insoluble fraction was removed by filtration and washed extensively with the mixture solvent and acetone. After determination of the insoluble part, $[\eta]$ of the soluble fraction was determined through Solomon-Ciuta equation using the corrected PET concentration.

Carboxyl content

The aged samples were dissolved in the mixture solvent and carboxyl content was determined by titration using bromophenol blue as indicator and KOH methanol solution as titrant.

Tensile test

Tensile test was conducted according to GB/T1040-92 using a testing machine (CMT5105, SANS, China) at room temperature at a crosshead speed of 10 mm·min^{-1}. Tensile strength and stain at break were reported as means from 5 duplicates for each samples.

Scanning electron microscopy (SEM)

The fracture surface morphology was examined using a scanning electron microscope (SEM, S-4800, Hitachi, Japan). Prior to the observations, the fracture surface was sputter-coated with a thin layer of gold to avoid electrical charging accumulating during examination.

RESULTS AND DISCUSSION

Morphology of PET/SiO_2 Nanocomposites

Figure 1 shows SEM morphology of PET and its nanocomposites. The cross-section of PET is smooth (Fig. 1a). In the nanocomposites, 0.5 wt% SiO_2 nanoparticles are well dispersed in PET (Fig. 1b). At 1.0 wt% SiO_2 content (Fig. 1c), most nanoparticles are homogeneously dispersed in the matrix, but there are some agglomerates with a maximum size of 400 nm. These agglomerates are formed due to relatively strong interactions between the surface silanol groups of fumed silica.

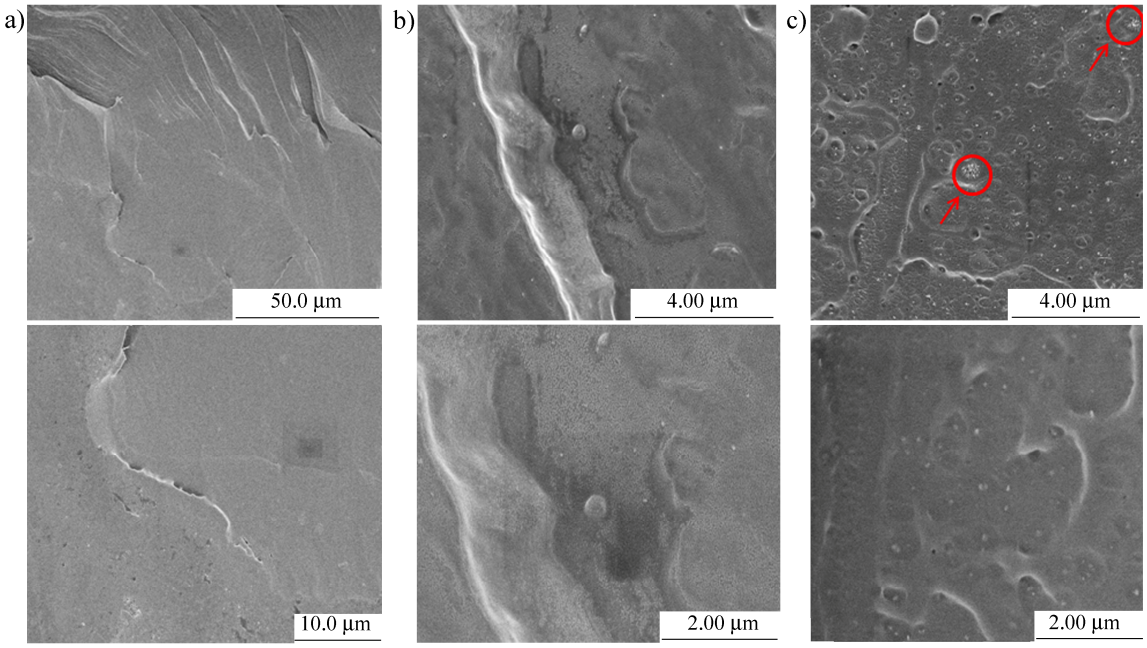


Fig. 1 SEM images of fracture surface of PET (a), PET-0.5 (b) and PET-1.0 (c)

Crystallization and Melting Behaviors of PET/SiO₂ Nanocomposites

Effect of SiO₂ content

Figure 2 shows DSC heating and cooling curves of PET and its nanocomposites. Glass transition (T_g) of PET gradually moves towards low temperatures with increasing SiO_2 content as reported in other studies[13, 38, 39]. The T_g depression could be ascribed the weakened intermolecular interaction or the reduced interparticle distance (PET film between silica particles). However, other observations[27, 29] show SiO_2 induced T_g rise, which is ascribed to restricted molecular mobility due to interfacial adsorption.

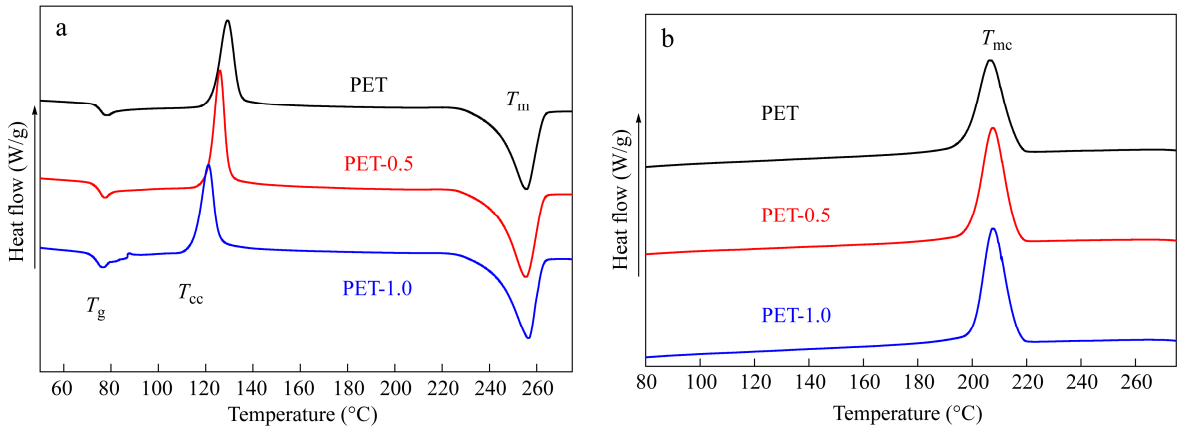


Fig. 2 DSC heating (a) and cooling curves (b) of PET and its nanocomposites

Cold crystallization temperature (T_{cc}) decreases (Fig. 2a) while melt crystallization temperature (T_{mc}) increases (Fig. 2b) with increasing SiO_2 content, which is in agreement with Ke *et al.*[28] and suggests SiO_2 has nucleation effect both in the cold and the melt crystallizations. It is well known that the molecular chains of pure PET present higher inflexibility and less mobility[27]. As a result, both crystallization rate and nucleation rate are very low. The incorporation of SiO_2 nanoparticles into the PET matrix enhances the crystallization rate by providing a large number of nucleation sites.

The melting and crystallization parameters are presented in Table 1. The melting enthalpy (ΔH_m) and melt crystallization enthalpy (ΔH_{mc}) are calculated from the areas of melting peak and melt crystallization peak, respectively, in DSC curves. The relative crystallinities (X_m and X_c for the melting and the melt crystallization processes, respectively) are determined using a melting enthalpy of 100% crystalline PET as 140 J/g[40]. As is seen in Table 1, SiO_2 does not significantly influence X_m and X_c. Rong *et al.* found the same tendency in polypropylene/SiO_2 composite[41]. SiO_2 also does not influence the T_m markedly.

Table 1. Crystallization parameters for PET and PET/silica composite samples

Sample	T_g (°C)	T_{cc} (°C)	T_m (°C)	ΔH_m (J·g^{-1})	X_m (%)	T_{mc} (°C)	ΔH_{mc} (J·g^{-1})	X_c (%)
PET	77.6	129.1	255.6	44.2	31.6	206.9	42.3	30.2
PET-0.5	77.1	126.1	255.4	46.7	33.3	207.6	43.1	30.7
PET-1.0	76.4	121.2	256.5	45.0	32.1	207.9	42.5	30.4

Isothermal crystallization

The effect of SiO_2 content on isothermal crystallization was examined at 240 °C, and the DSC curves are shown in Fig. 3. Characteristic crystallization times are listed in Table 2. The crystallization peak becomes sharp with increasing SiO_2 content and the peak exothermal time (t_p) decreases obviously. The crystallization induction period (t_{ind}) and half-time ($t_{1/2}$) decrease, respectively, from 15.7 min and 34.4 min of pure PET to 10.5 min and 28.4 min at 1.0 wt% SiO_2, suggesting again that SiO_2 accelerates the isothermal crystallization[27].

Table 2. Characteristic times for isothermal crystallization of PET and its nanocomposites at 240 °C

Sample	$t_{1/2}$ (min)	t_{ind} (min)	t_p (min)
PET	34.4	15.7	45.1
PET-0.5	32.8	13.7	44.3
PET-1.0	28.4	10.5	39.6

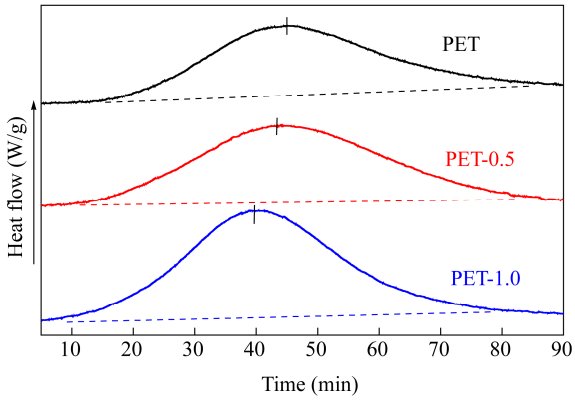


Fig. 3 DSC curves of PET and its nanocomposites isothermally crystallized at 240 °C

The effect of SiO_2 on spherulite morphology during isothermal crystallization was examined using POM, as shown in Fig. 4. As SiO_2 content increases from 0 wt% to 1 wt%, crystal nuclei density increases significantly and the spherulite size decreases due to the improved nucleating ability of PET[27].

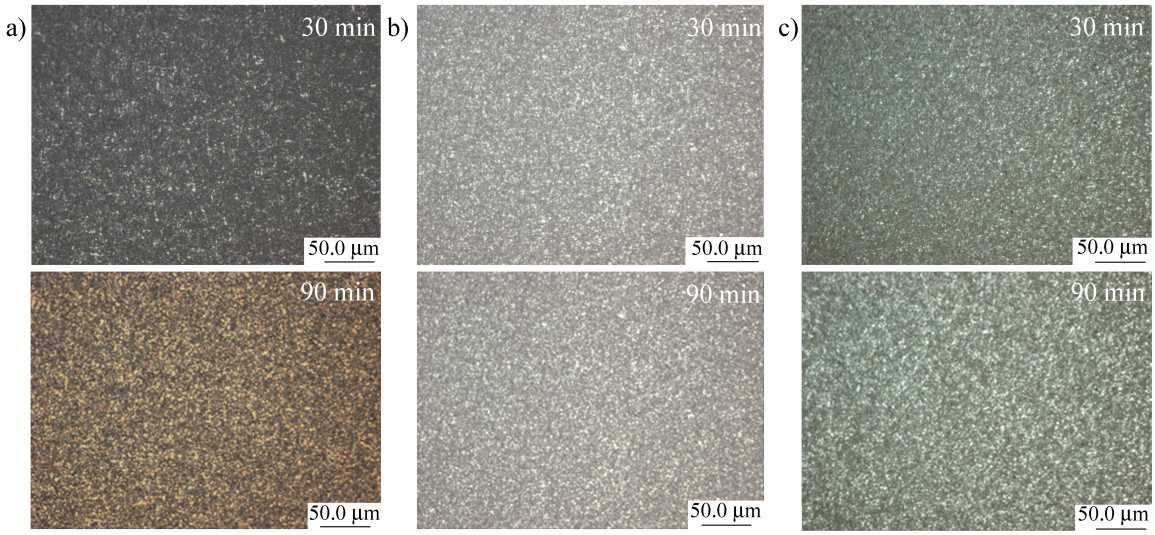


Fig. 4 POM pictures taken from films of PET (a), PET-0.5 (b) and PET-1.0 (c) duringisothermal crystallization at 240 °C for 30 min and 90 min after melting at 290 °C

Figure 5 shows relative crystallinity (X_t) as a function of time (t) for PET and PET-1.0. The curves move towards longer crystallization time at higher temperatures due to the improved molecular mobility and the lower nucleation density while $t_{1/2}$ of PET-1.0 at each temperature is approximately 26.0% shorter than that of PET.

Avrami equation was used to analyze the crystallization dynamics, and the parameters are summarized in Table 3. Avrami index (n) for both PET and PET-1.0 is located at 2.2–2.9, revealing a three-dimensional crystal growth. In comparison with PET, crystallization rate (G) of PET-1.0 is 40% in average higher than that of PET.

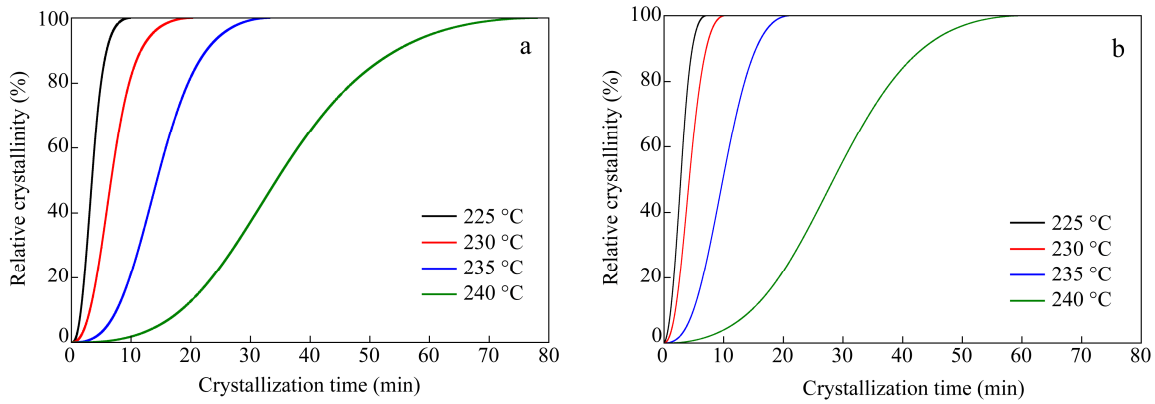


Fig. 5 Relative crystallinity versus time for PET (a) and PET-1.0 (b) crystallized from melt at 225 °C, 230 °C, 235 °C and 240 °C

Table 3. Avrami parameters for isothermal crystallization of PET and PET-1.0

Sample	T_c (°C)	n	LgK (min^{-n})	$t_{1/2}$ [a] (min)	G [b] (min^{-1})
PET	225	2.41	–1.45	3.44	0.29
	230	2.40	–2.14	6.66	0.15
	235	2.87	–3.48	14.34	0.07
	240	2.87	–4.57	34.41	0.03
PET-1.0	225	2.20	–1.15	2.78	0.36
	230	2.35	–1.63	4.23	0.24
	235	2.68	–2.82	9.86	0.10
	240	2.91	–4.38	28.41	0.04

[a] $t_{1/2}=(\ln 2/k)^{1/n}$; [b] $G=(t_{1/2})^{-1}=(\ln 2/k)^{-1/n}$

Non-isothermal crystallization

The non-isothermal crystallization DSC curves are presented in Fig. 6. With increasing cooling rate Φ, the crystallization peak shifts to lower temperatures[28]. At slow cooling rates, the molecular chains have enough time to pack up in a unit cell to form crystalline phase rapidly. Jeziorny equation was used to analyze the non-isothermal crystallization and the results are summarized in Table 4. At the primary stage of the non-isothermal crystallization, G increases with increasing Φ for PET and PET-1.0. PET-1.0 exhibits G higher than that for PET at given Φ due to SiO_2 accelerating the crystallization.

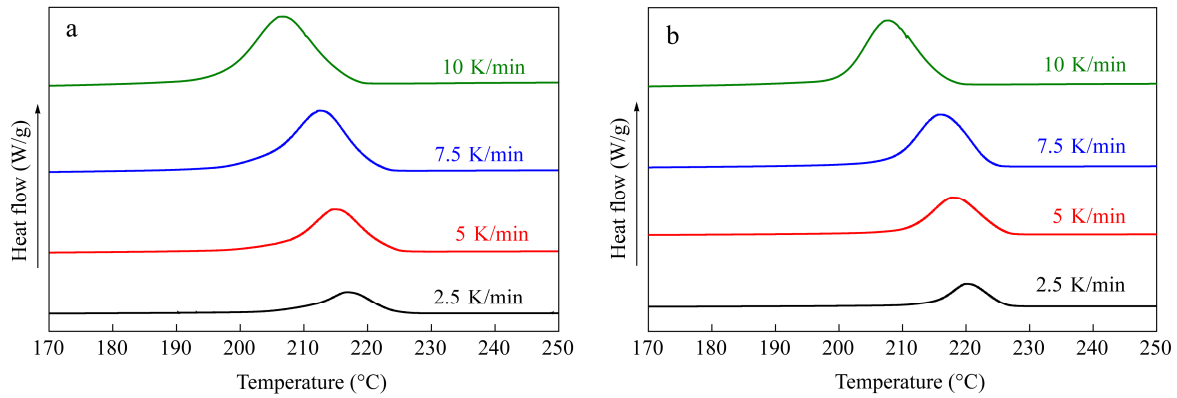


Fig. 6 Non-isothermal crystallization curves for PET (a) and PET-1.0 (b) at different cooling rates

Table 4. Kinetic parameters for PET and PET-1.0 under non-isothermal crystallization

Sample	Φ (°C/min)	n	lg(Z_t) [a] (min^{-n})	G [b] (min^{-1})
PET	2.50	4.61	–0.61	1.03
	5.00	4.43	1.18	1.15
	7.50	3.51	1.74	1.18
	10.0	2.99	1.99	1.21
PET-1.0	2.50	5.54	–0.31	1.05
	5.00	4.85	1.38	1.16
	7.50	3.43	2.03	1.20
	10.0	2.89	2.08	1.23

[a] $G = (\ln 2/Z_c)^{-1/n}$; [b] $\lg Z_c = \lg Z_t/\Phi$

According to the theory of Avrami, Avrami index shall be equal to the sum of space dimension of the crystal growth and time dimension of nucleation. As shown in Table 3, at the primary stage of isothermal crystallization, n increases with increasing T_c for both PET and PET-1.0. It means that the nucleation is more dependent on time. It might be because PET has a low energybarrier of nucleation at low temperatures, so most of nucleates can be formed in a short time period and the nucleation is less dependent on time at low temperatures. On the other hand, at high temperatures, PET has a high energy barrier of nucleation so that the nucleation is more dependent on time, leading to the n value increase.

For non-isothermal crystallization of PET, course of crystallization needs some time, at low cooling rate Φ, the whole process of crystallization occurs mainly at high temperatures. On the contrary, at high cooling rate Φ, the whole process of crystallization occurs mainly at low temperatures. Thus, as shown in Table 4, n declines with increasing cooling rate Φ.

Ageing Behavior

[η] and carboxyl index

In order to understand the effects of SiO_2 on the ageing properties of PET and its nanocomposites, a series of studies of thermal treatment were carried out at 190 °C in air environment for different time. Figure 7 shows [η] and carboxyl contentversus ageing time. [η] gradually declines and carboxyl content increases with ageing time, which confirms the PET degradation leads to the formation of carboxyl end groups[42, 43]. However, the variations of [η] and carboxyl content of the nanocomposites are smaller than those of pure PET and the PET-0.5 exhibits the slowest rate of degradation.

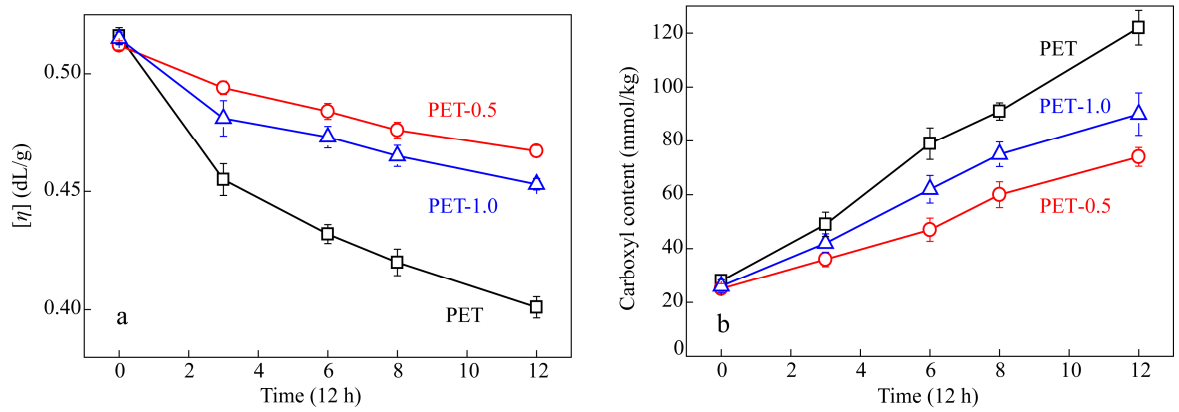


Fig. 7 Intrinsic viscosity [η] (a) and carboxyl content (b) as a function of aging time for PET and its nanocomposites at 190 °C

Tensile properties

Room temperature tensile properties of PET and its nanocomposites were investigated after ageing at 190 °C for different times, and the results are shown in Fig. 8. Aging causes significant reductions in tensile strength and

elongation at break. However, the presence of SiO_2 could weaken the effect of aging on tensile strength. Tensile strength of PET reduces by 58.3% while that of PET-0.5 and PET-1.0 decreases by 39.2% and 44.0% after aging for 6 days, respectively. Pure PET and its nanocomposites exhibit a great reduction in elongation at break by 99.2%–99.5% after aging for 6 days. The degradation in tensile properties mainly occurs in the early stage of aging, which might be resulted from cold crystallization at the aging temperature located between T_{cc} and T_m. On the other hand, in the thermal oxidation conditions, molecular degradation also occurs gradually[44, 45], which partially contributes to the degradation in tensile properties and accounts for the variations of $[\eta]$ and carboxyl content as shown in Fig. 7.

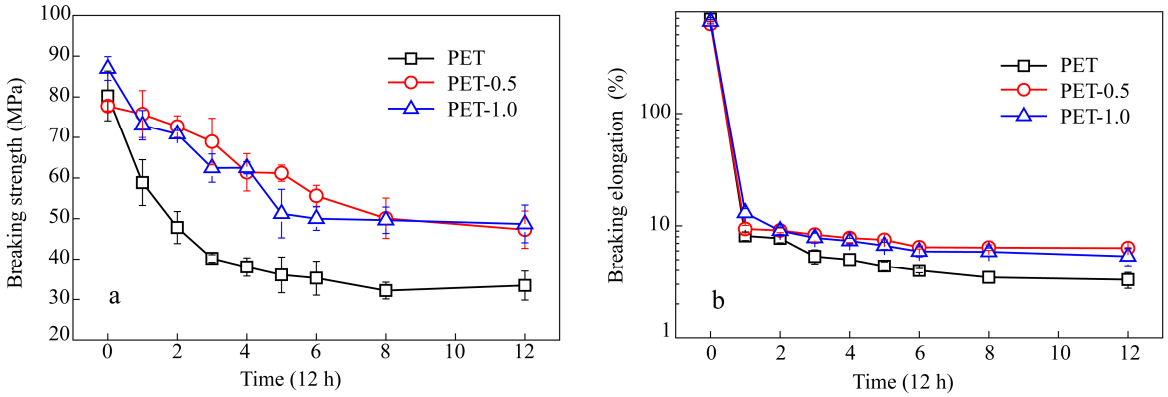
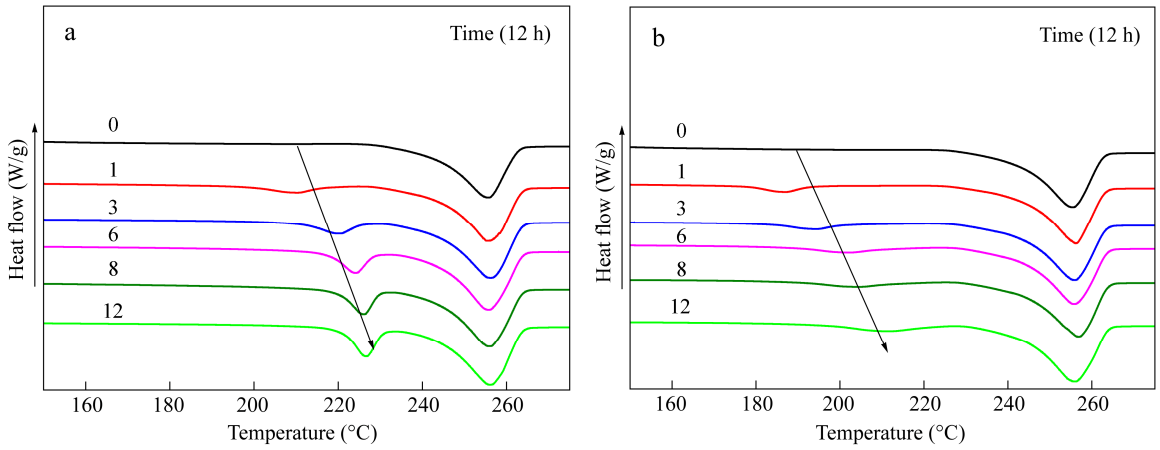


Fig. 8 Room temperature tensile strength (a) and elongation at break (b) as a function of aging time for PET and its nanocomposites during aging at 190 °C

Crystallization behavior

Aging influences the crystallization behavior of PET and its nanocomposites. Figure 9 shows DSC curves of the aged samples. There are two endothermic peaks appeared in the aged samples and the small one at lower temperature (T_{m1}) shifts to higher temperatures with increasing aging time while the large one located at T_{m2} = 256 °C is independent of aging. T_{m2} is the same as the unaged samples and reflects the melting of normal PET crystals. The PET macromolecules degraded into small molar mass generally favors the formation of small crystals responsible for the appearance of T_{m1}. Figure 10 shows T_{m1} and its associated endotherm as a function of aging time for PET and its nanocomposites. Both T_{m1} and its associated endotherm increase with increasing aging time, suggesting an effect of thermal induced crystal growth together with the molecular degradation. The presence of SiO_2 causes a reduction in T_{m1} and its associated endotherm at given aging time and the effect is more marked at 0.5 wt% SiO_2. The results may be related to the SiO_2 lessening the thermal degradation of PET.



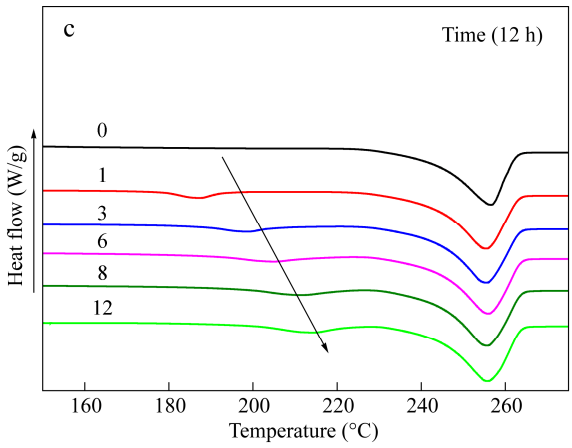


Fig. 9 Heating DSC scans of PET (a), PET-0.5 (b) and PET-1.0 (c)

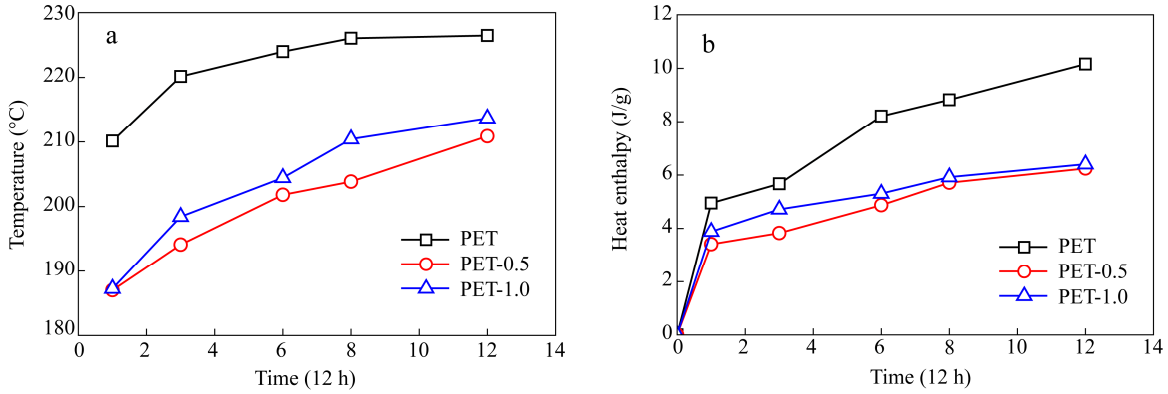


Fig. 10 T_{m1} (a) and its associated endotherm (b) as a function of aging time for PET and its nanocomposites

SEM micrographs

Figure 11 shows SEM micrographs of fracture surfaces of PET and it nanocomposites after ageing for 6 days. Before ageing, all samples exhibit a smooth fracture surface. After ageing, the samples exhibit a rough surface with microvoids associated with degradation of PET. The size of microvoids in the aged samples ranks in an order of PET > PET-0.5 > PET-1.0. Although the incorporation of SiO_2 has little effect on the degree of crystallinity of PET, the nucleating ability of PET is highly improved by SiO_2 to form fine crystals with reduced size compared with those of pure PET. The fine crystals form compact network to enhance oxygen and moisture barrier properties and reduce the permeability, which provides an explanation for the retarded degradation during aging of PET in presence of SiO_2. To analyze the unexpected increase of PET degradation rate with more SiO_2 added, SEM micrographs of fracture surfaces of PET-1.0 after ageing 6 days are shown in inset in Fig. 11(c). As depicted in Fig. 11(c), the cracks at the silica/matrix interfaces can be observed after ageing, revealing the another possible degradation mechanism might be the damage of the silica/matrix interface.

The PET decomposition at the silica/matrix interface can be possibly classified into two kinds. (a) There are a large number of hydrophilic hydroxyls on the surface of SiO_2, generating an effective interaction with H_2O. Therefore, the addition of SiO_2 can adsorb more moisture in the air, leading to faster hydrolysis of ester groups in PET. (b) The thermal expansion coefficient of PET is higher than SiO_2. When the nanocomposites are aged at 190 °C, the matrix expands much more than SiO_2 to form microcracks at the silica/matrix interface, resulting in accessional diffusion of oxygen and moisture from the air to the polymer matrix, and accelerating the degradation of PET.

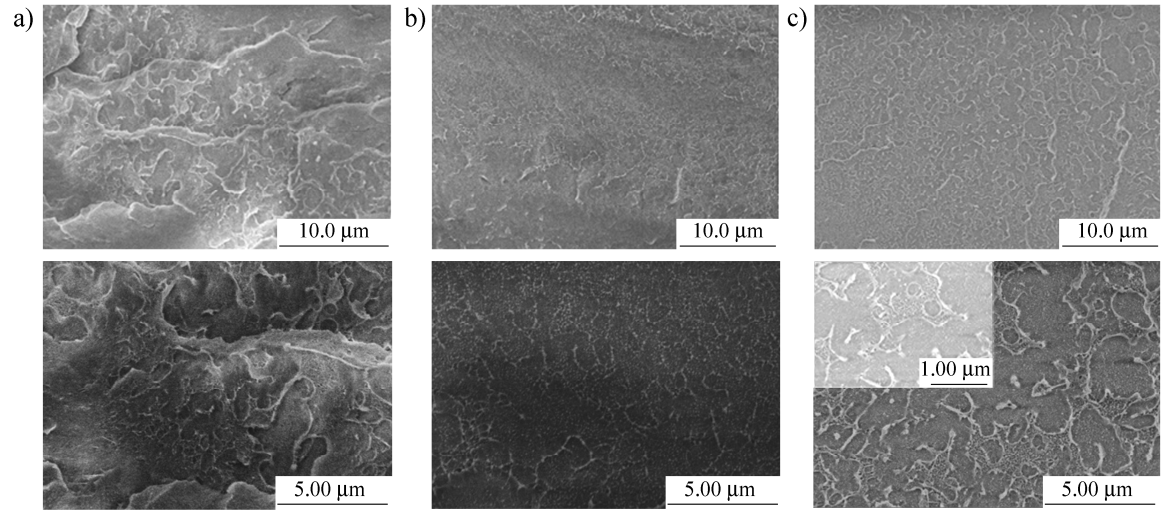


Fig. 11 SEM micrographs of fracture surfaces of PET (a) and it nanocomposites with 0.5 wt% (b) and 1.0 wt% SiO_2 (c) after ageing at 190 °C for 6 days (The inset in (c) shows micrograph of PET-1.0 after ageing for 6 days.)

The results indicate clearly that SiO_2 has a dual effect on PET degradation. On one hand, the network of crystals becomes more compact, which enhances the oxygen and moisture barrier properties, and delays the degradation rate with increasing SiO_2 content. On the other hand, the addition of SiO_2 leads to a promoted PET degradation at the SiO_2/matrix interfaces. The barrier effect is more dominant than the catalysis factor of SiO_2 on degradation so that the nanocomposites have considerably enhanced anti-degradation properties compared with neat PET films. However, at considerably high SiO_2 contents, the catalysis effect of SiO_2 on degradation is enhanced greatly, leading to the reduction of anti-degradation properties.

Therefore, results from tensile properties, $[\eta]$ and carboxyl content reveal that PET-0.5 with a fine silica dispersion exhibits a lower degradation rate than PET and PET-1.0.

CONCLUSIONS

Both non-isothermal and isothermal crystallization results indicate that SiO_2 could promote the melt-crystallization without significant influence on relative crystallinity of PET. The investigations by tensile properties, $[\eta]$ and carboxyl content reveal that addition of SiO_2 could reduce the degradation rate of PET and the effect is more marked at 0.5% SiO_2 with fine dispersion in the matrix.

REFERENCES

1 Wu, D., Chen, F., Li, R. and Shi, Y., Macromolecules, 1997, 30(22): 6737
2 Reinsch, V.E. and Rebenfeld, L., J. Appl. Polym. Sci., 1994, 52(5): 649
3 Pilati, F., Toselli, M., Messori, M., Manzoni, C., Turturro, A. and Gattiglia, E., Polymer, 1997, 38(17): 4469
4 Hosseini, S.S., Taheri, S., Zadhoush, A. and Mehrabani-Zeinabad, A., J. Appl. Polym. Sci., 2007, 103(4): 2304
5 Marini, M., Pilati, F., Saccani, A. and Toselli, M., Polym. Degrad. Stab., 2008, 93(6): 1170
6 Al-Abdul Razzak, S. and Jabarin, S.A., Polym. Int., 2002, 51(2): 164
7 Gregory, D. and Watson, M., Polym. Eng. Sci., 1972, 12(6): 454
8 Wampler, F.C. and Gregory, D.R., J. Appl. Polym. Sci., 1972, 16(12): 3253
9 Wu, B., Wang, Y.Z., Wang, X.L., Yang, K.K., Jin, Y.D. and Zhao, H., Polym. Degrad. Stab., 2002, 76(3): 401
10 Jordan, J., Jacob, K.I., Tannenbaum, R., Sharaf, M.A. and Jasiuk, I., Mater. Sci. Eng., A, 2005, 393(1–2): 1

11 Hopkinson, I., Myatt, M. and Tajbakhsh, A., Polymer, 2004, 45(12): 4307
12 Nam, P.H., Maiti, P., Okamoto, M., Kotaka, T., Hasegawa, N. and Usuki, A., Polymer, 2001, 42(23): 9633
13 Todorov, L.V. and Viana, J.C., J. Appl. Polym. Sci., 2007, 106(3): 1659
14 Taniguchi, A. and Cakmak, M., Polymer, 2004, 45(19): 6647
15 Aoyama, S., Park, Y.T., Ougizawa, T. and Macosko, C.W., Polymer, 2014, 55(8): 2077
16 Ou, Y., Yang, F. and Yu, Z.Z., J. Polym. Sci., Part B: Polym. Phys., 1998, 36(5): 789
17 Ji, Q., Wang, X., Zhang, Y., Kong, Q. and Xia, Y., Composites Part A, 2009, 40(6): 878
18 Münstedt, H., Köppl, T. and Triebel, C., Polymer, 2010, 51(1): 185
19 Li, M. and Jeong, Y.G., Composites Part A, 2011, 42(5): 560
20 Vassiliou, A.A., Chrissafis, K. and Bikiaris, D.N., Thermochim. Acta, 2010, 500(1–2): 21
21 Wang, Y., Gao, J., Ma, Y. and Agarwal, U.S., Composites Part B, 2006, 37(6): 399
22 Xu, X., Ding, Y., Wang, F., Wen, B., Zhang, J., Zhang, S. and Yang, M., Polym. Compos., 2010, 31(5): 825
23 Alongi, J., Ciobanu, M., Tata, J., Carosio, F. and Malucelli, G., J. Appl. Polym. Sci., 2011, 119(4): 1961
24 Wu, T. and Ke, Y., Polym. Degrad. Stab., 2006, 91(9): 2205
25 Zheng, J., Cui, P., Tian, X. and Zheng, K., J. Appl. Polym. Sci., 2007, 104(1): 9
26 Kusuktham, B., J. Appl. Polym. Sci., 2012, 126(S2): E387
27 Yang, Y., Xu, H. and Gu, H., J. Appl. Polym. Sci., 2006, 102(1): 655
28 Ke, Y.C., Wu, T.B. and Xia, Y.F., Polymer, 2007, 48(11): 3324
29 He, J.P., Li, H.M., Wang, X.Y. and Gao, Y., Eur. Polym. J., 2006, 42(5): 1128
30 Zhu, Y.G., Li, Z.Q., Zhang, D. and Tanimoto, T., J. Polym. Sci., Part B: Polym. Phys., 2006, 44(9): 1351
31 Turturro, G., Brown, G.R. and St-Pierre, L.E., Polymer, 1984, 25(5): 659
32 Antoniadis, G., Paraskevopoulos, K., Bikiaris, D. and Chrissafis, K., Thermochim. Acta, 2010, 510(1): 103
33 Zheng, H. and Wu, J., J. Appl. Polym. Sci., 2007, 103(4): 2564
34 Avrami, M., J. Chem. Phys., 1939, 7: 1103
35 Avrami, M., J. Chem. Phys., 1940, 8: 212
36 Jeziorny, A., Polymer, 1978, 19(10): 1142
37 Solomon, O. and Ciută, I., J. Appl. Polym. Sci., 1962, 6(24): 683
38 Ash, B.J., Schadler, L.S. and Siegel, R.W., Mater. Lett., 2002, 55(1–2): 83
39 Becker, C., Krug, H. and Schmidt, H., MRS Proceedings, 1996, 435: 237
40 Mehta, A., Gaur, U. and Wunderlich, B., J. Polym. Sci., Part B: Polym. Phys., 1978, 16(2): 289
41 Rong, M.Z., Zhang, M.Q., Zheng, Y.X., Zeng, H.M., Walter, R. and Friedrich, K., Polymer, 2001, 42(1): 167
42 Foulc, M., Bergeret, A., Ferry, L., Ienny, P. and Crespy, A., Polym. Degrad. Stab., 2005, 89(3): 461
43 Blasi, P., D'Souza, S.S., Selmin, F. and DeLuca, P.P., J. Control. Release, 2005, 108(1): 1
44 Flory, P.J., J. Am. Chem. Soc., 1945, 67(11): 2048
45 Vincent, P., Polymer, 1960, 1: 425